

Production rate determines plasma concentration of large high density lipoprotein in non-human primates

Perry Colvin,^{1,†} Emilio Moriguchi,^{2,*} Hugh Barrett,[§] John Parks,* and Larry Rudel*

Department of Comparative Medicine,* Wake Forest University School of Medicine, Winston-Salem, NC 27157; Department of Internal Medicine,[†] Division of Gerontology, University of Maryland School of Medicine and the Baltimore Veterans Affairs Medical Center, Geriatrics Research, Education, and Clinical Center, Baltimore, MD 21201; and Department of Bioengineering,[§] University of Washington, Seattle, WA 98195

Abstract Large LpAI HDL particles, containing only apoA-I without apoA-II, are reported to be the major anti-atherogenic portion of HDL and to be increased in individuals with low risk for coronary heart disease. To determine whether the plasma concentration of large LpAI is modulated by the rate of production or catabolism of apolipoprotein A-I (apoA-I) in large LpAI, kinetic studies of large LpAI were performed in African green monkeys consuming an atherogenic diet with either high plasma HDL concentration (120 ± 36 mg/dl, mean \pm SD, $n = 3$) or low plasma HDL concentration (40 ± 13 mg/dl, $n = 3$). Large LpAI was isolated, without ultracentrifugation, by immunoaffinity and gel filtration and radiolabeled. After injection, the specific activity of apoA-I in large HDL, consisting of both LpAI and LpAI:AI particles, was followed. A multicompartmental model was developed for the kinetics of apoA-I in large HDL, which indicated that a portion of large HDL is distributed to a sequestered pool, outside the circulating plasma, and reenters circulating plasma approximately 3 h after injection. There was no conversion of large LpAI to smaller HDL particles or transfer of radiolabeled apoA-I to smaller HDL particles. Although the mean fractional catabolic rate was not different comparing the high and low HDL group, the mean production rate of apoA-I in large HDL was 4-fold greater in the high HDL group compared with the low HDL group. These data support the hypothesis that the plasma concentration of large HDL is controlled primarily by the rate of production of apoA-I in large HDL.—Colvin, P., E. Moriguchi, H. Barrett, J. Parks, and L. Rudel. Production rate determines plasma concentration of large high density lipoprotein in non-human primates. *J. Lipid Res.* 1998. 39: 2076–2085.

Supplementary key words high density lipoprotein • LpAI • LpAI:AI • apoA-I • apoA-II • catabolism • kinetic model

High density lipoproteins (HDL) are the smallest of the plasma lipoprotein classes and display significant heterogeneity in size and density (1). HDL subfractions can be separated by size (2, 3), density (4), electrophoretic mobility (5), and apolipoprotein (apo) content (6). HDL are thought to play an important role in reverse cholesterol

transport, a process in which excess free cholesterol in peripheral tissues is incorporated into HDL in plasma, esterified by lecithin:cholesterol acyltransferase (LCAT), and then transported to the liver for subsequent secretion into bile as cholesterol or bile acid (7). This process is hypothesized to reduce the amount of excess cholesterol in arterial tissue, resulting in less atherosclerosis and may explain the inverse relationship between HDL cholesterol concentrations and 1) development of coronary heart disease (CHD) in human subjects (8, 9) and 2) development of coronary artery atherosclerosis in monkeys (10, 11). Transgenic mice overexpressing human apolipoprotein A-I have higher HDL concentrations and develop less atherosclerosis than control mice (12). These observations in humans and experimental animals have supported the hypothesis that HDL are anti-atherogenic and have stimulated interest in understanding the metabolism of HDL.

Recent studies have focused on the use of immunoaffinity chromatography as a method for preparative isolation of HDL that avoids the modification of HDL caused by ultracentrifugation (13). Two major classes of HDL have been the subject of study, one that contains apoA-I without apoA-II (LpAI) and one that contains both apoA-I and apoA-II (LpAI:AI) (14). LpAI concentrations are inversely proportional to the prevalence of CHD in man and transgenic mice with elevated concentrations of LpAI develop less atherosclerosis compared to those with elevated concentrations of LpAI:AI (15, 16). LpAI is also more efficient at removing excess cholesterol from cells in culture compared to LpAI:AI (17, 18). These results taken to-

Abbreviations: LpAI, large HDL particles containing only apoA-I; HDL, high density lipoproteins; CHD, coronary heart disease; LCAT, lecithin:cholesterol acyltransferase; apo, apolipoprotein.

¹To whom correspondence and reprint requests should be addressed.

²Current address: Geriatrics Institute, Pontifical Catholic University of Rio Grande do Sul, Brazil.

gether suggest that LpAI are more protective against atherosclerosis development than LpAI:AI.

About 65% of the apoA-I in human plasma is associated with LpAI:AI particles, whereas 25% is on LpAI particles (17). ApoA-I on LpAI has a faster catabolic rate than apoA-I on LpAI:AI (19); however, there is little information regarding the size distribution of LpAI. One study that examined the distribution and composition of LpAI in normolipidemic men and women demonstrated that higher HDL concentrations in women were due to an increase in large and a decrease in medium LpAI particles compared to men (20). However, there were no compositional differences in large, medium, or small LpAI particles between men and women.

Several studies have demonstrated a faster catabolic rate for apoA-I in subjects with low HDL versus high HDL concentrations (21, 22). Subjects with low HDL tended to have smaller HDL and a greater fraction of apoA-I isolated in the $d > 1.21$ g/ml fraction after ultracentrifugation, suggesting that apoA-I on these particles are less stable during ultracentrifugation than apoA-I on particles from subjects with high HDL concentrations. This conclusion was supported by rat kidney perfusion studies which showed that HDL from individuals with low concentrations had a greater percentage of apoA-I that was taken up by the kidney compared to HDL from subjects with high concentrations (21). Comparable metabolic studies have not been reported of un-ultracentrifuged LpAI in individuals with high versus low HDL concentrations.

The purpose of the present study was to determine whether individual differences in plasma HDL concentrations of non-human primates consuming an atherogenic diet were related to catabolism of LpAI particles. We hypothesized that animals with high HDL concentrations would have a greater proportion of large LpAI, analogous to the situation in women, compared to those with low HDL concentrations. The greater proportion of LpAI particles in plasma could result from a delayed catabolism of these particles in animals with high HDL concentrations. Alternatively, the production rate of large LpAI particles may be greater in animals with high plasma HDL concentrations. We report here the results of kinetic studies using large LpAI tracers isolated by gel filtration and sequential immunoaffinity chromatography in six African green monkeys: three with plasma LpAI concentrations of 34.5 ± 26.5 mg/dl (mean \pm SD) and three with mean plasma LpAI concentration of 131.1 ± 39.8 mg/dl.

METHODS

Animals

Six recipient adult male African green monkeys were used for this study. The study animals were selected from an ongoing experiment (23) in which animals were fed an atherogenic diet consisting of 35% of calories as fat (lard) and either 0.4 or 0.8 mg cholesterol/kcal. In an attempt to maximize the differences in the high and low HDL cholesterol groups, animals for this study

were chosen from both diet groups. Two recipient monkeys consumed the 0.4 mg cholesterol/kcal diet (one monkey in the low HDL group and one in the high HDL group). The remaining four recipient monkeys consumed the 0.8 mg cholesterol/kcal diet. The average daily consumption was 90 kcal/kg weight. The animals had consumed the experimental diet for at least 5 years before the metabolic studies were performed. The six recipient study animals were selected from a group of 24 monkeys to establish two experimental groups with either low or high plasma HDL cholesterol concentrations (Table 1). Mean body weight was 4.09 kg for the low HDL group and 4.60 kg for the high HDL group. All animals were individually housed in an enriched environment in the animal facility at the Wake Forest University School of Medicine, which is approved by the American Association for the Accreditation of Laboratory Animal Care and supervised by a veterinary staff. All procedures were approved by the Institutional animal care and use committee.

Isolation of LpAI

For the preparation of the tracer LpAI, blood was drawn from the femoral vein of two donor animals restrained by injection of ketamine HCl (10 mg/kg) after they had been fasted overnight. The donor animals were fed the 0.8 mg cholesterol/kcal diet. Plasma was promptly isolated from the blood by centrifugation at 2,000 *g* for 30 min at 4°C in the presence of the following preservatives and inhibitors: 0.01% EDTA, 0.01% NaN₃, 10 kallikrein inhibitor units of aprotinin/ml, and 0.08 mg PMSF/ml (final concentration). Plasma (10 ml) was applied to an 8% agarose column (2.5 × 90 cm) and lipoproteins were separated and eluted with 0.15 M NaCl, 0.01% EDTA, 0.01% NaN₃, pH 7.4 (column buffer) at 4°C. The distribution of the lipoproteins eluted from the column and collected in a fraction collector was evaluated by the measurement of total cholesterol and apolipoproteins A-I, A-II, B, and E in each of the column fractions. ApoA-I-containing fractions were pooled in 3 different size ranges; large, medium, and small as the front, middle, and back portions of the apoA-I peak eluted from the column (Fig. 1).

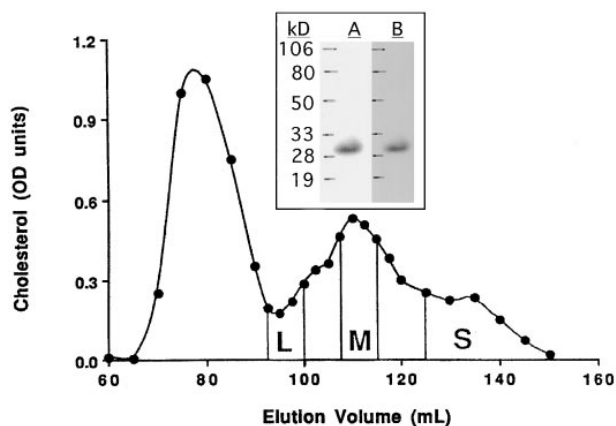


Fig. 1. Elution profile of monkey plasma on 8% agarose column. Individual fractions were assayed for cholesterol using an enzymatic assay (29) and optical density units are plotted versus elution volume. The apoA-I-containing region of the column elution profile, determined by ELISA assay, was pooled into large (L), medium (M), and small (S) particles. The inset shows the results of SDS polyacrylamide gradient gel (4–30%) electrophoresis of tracer large LpAI after immunoaffinity isolation and radioiodination. Lane A shows the Coomassie blue stained-gel and lane B shows the autoradiography of the gel. Molecular weight markers are shown on the left side of the insert.

LpAI and LpAI:AII were isolated from the large HDL regions from the 8% agarose column eluate. Antisera to purified monkey apoA-I and apoA-II (24) was raised in goats as previously described (25). Antibodies mono-specific for apoA-I and apoA-II were isolated from the respective antisera by affinity chromatography using an African green monkey whole serum column, after purification of the IgG by ammonium sulfate precipitation (26). The immunoaffinity-purified antibodies were coupled to Affi-gel 10 (Bio-Rad) according to the manufacturer's directions. The immunoaffinity columns were equilibrated with 0.01 M Na phosphate, 0.15 M NaCl, pH 7.4 (PBS) before use. The size-fractionated HDL samples from the 8% agarose column were applied to the anti-A-II column; the column was washed with PBS until the absorbance at 280 nm was <0.001 , and the bound particles were eluted with 3 M NaSCN, pH 7.4, and immediately desalted over an 80-ml Sephadex G-25 medium coarse column, equilibrated with column buffer. The eluted LpAI:AII fraction was dialyzed against column buffer and concentrated to 1 ml in Centriflo CF25 membrane cones (Amicon). The flow through from the anti-A-II column was applied to the anti-A-I column; the column was washed, and the LpAI particles were eluted, desalted, dialyzed, and concentrated as described above for the LpAI:AII particles. Aliquots of bound and unbound fractions from each column run were assayed for apoA-I and apoA-II concentrations using a sandwich enzyme-linked immunosorbent assay (ELISA) (26). The ELISA procedures for the measurement of apoA-II and apoE were essentially the same as described for apoA-I (26) using the respective monospecific immunopurified antibodies. Recovery from the immunoaffinity columns ranged from 90 to 95%.

Lipoprotein characterization

Protein was measured by the method of Lowry et al. (27), and phospholipid was quantified by a modification of the method described by Rouser, Fleischer, and Yamamoto (28). Triglyceride, free and total cholesterol concentrations were determined using enzymatic assays (29), after extraction of the lipoprotein particles according to the method of Bligh and Dyer (30).

SDS polyacrylamide gradient gel (4–30%) electrophoresis was performed as described (29). After electrophoresis, the gels were fixed for 2 h with 25% isopropanol, 10% acetic acid, and washed for 1 h with 7.5% acetic acid before autoradiography or quantification of radioactivity in gel slices.

Lipoprotein particle size distribution was determined by 4–30% non-denaturing gradient gel electrophoresis ($1400V \times h$ at $10^\circ C$) as described previously (31, 32). For determination of apoA-I distribution among LpAI of different sizes, the proteins were electrophoretically transferred from the 4–30% non-denaturing gradient gels to nitrocellulose membranes (0.45 μm , Schleicher & Schuell, Keene, NH) in 0.192 M glycine, 0.025 M Tris, pH 8.5, for a total of $840V \times h$ at $10^\circ C$. The nitrocellulose blots were then blocked with 5% non-fat dry milk in 0.02 M NaCl, 0.01 M Tris/HCl, pH 7.40 (TS) for 2 h at room temperature. The blots were treated with a 1:250 dilution of goat anti-monkey apoA-I or 1:100 dilution of goat anti-monkey apoA-II antisera in 2.5% non-fat dry milk, 0.1% Triton X-100, 0.02% SDS in TS (antibody buffer) for 1.5 h at room temperature. The blots were washed 4×20 min each with TS containing 0.1% Triton X-100, 0.02% SDS (wash buffer) at room temperature and incubated with a 1:2,000 dilution of alkaline phosphatase anti-goat IgG (Vector, Burlingame, CA) in antibody buffer for 2 h at room temperature. The blots were then washed for 20 min in wash buffer, followed by three successive 20-min washes with TS. ProtoBlot[®] NBT and BCIP Color Development System (Promega, Madison, WI) were used to develop the blots according to the manufacturer's instructions.

Iodination of LpAI

LpAI was iodinated with carrier-free ^{125}I according to the method of McFarlane (33), as modified by Bilheimer, Eisenberg, and Levy (34). Specific activities ranged from 350 to 1500 cpm/ng protein.

The iodinated apoA-I-containing particles were subjected to a second size exclusion chromatography step using a 10% agarose column (16/100 mm; Bio-Gel A-0.5m, 200–400 mesh, Bio-Rad) equilibrated with column buffer and then extensively dialyzed to remove any free iodide. This step was necessary to obtain homogeneous large LpAI particles for reinjection. Figure 1 shows a representative SDS-PAGE and autoradiography of the large LpAI tracer. SDS-PAGE and autoradiography indicated that only apoA-I was present in the LpAI tracer. No apoA-II or apoE was detected in the LpAI tracer.

Cross-linking studies of the isolated apoA-I-containing particles were performed to determine the number of apoA-I molecules per particle using the dimethylsuberimidate (DMS) method of Swaney and O'Brien with slight modification (35). Briefly, isolated iodinated samples were incubated with freshly prepared DMS solution (20 mg DMS dissolved in 1 ml of 1 M triethanolamine HCl, pH 9.7) in a proportion of 1 part of DMS solution to 2 parts of apoA-I solution. The reaction was carried out at room temperature for 2 h and terminated by the addition of 1 part of 20% SDS solution. Cross-linked samples were then adjusted to 10% sucrose (w/v), loaded onto pre-equilibrated 4–30% SDS gradient gels, electrophoresed, and fixed as described above. The gel was then subjected to autoradiography to visualize the size distribution of the radiolabeled dose.

In vivo metabolic studies

Recipient animals were jacket trained for several weeks before initiation of the in vivo metabolic studies. The reinjection studies were performed in pairs, with a low and high plasma HDL recipient. Femoral artery and vein cannulas of silastic tubing (0.04 I.D. \times 0.085 O.D. in) were surgically implanted, at least 2 days before the reinjection studies, for blood sampling of unanesthetized animals (36). The cannulas exited the cage through a stainless steel swiveled tether system connected to the monkey jacket. A solution of 0.45% NaCl, 0.05% NaI was given ad libitum to recipient animals 1 week prior and throughout the study period to block thyroid uptake of radiolabeled iodine. On the first morning (~ 9 am) of the study, ^{125}I -labeled large LpAI (100–200 μg protein) was injected into the femoral vein of animals fasted overnight and 1.5-ml blood samples were collected at: 5, 10, 15, 30, 45 minutes and 1, 1.5, 2, 2.5, 3, 4, 6, 9, 12, 24, 36, 48, 72, 96, 120, 144, 168, and 192 h after injection. Blood samples were collected into chilled tubes containing 0.1% EDTA, 0.01% NaN₃, 10 kallikrein inhibitor units apoprotein/ml, and 0.08 mg PMSF/ml and placed on ice. The cannulas were kept patent with a slow (~ 2 ml/h) infusion of 0.9% NaCl. On the first day of the metabolic studies, the fasted recipient animals were not fed their usual morning meal but were returned to their normal 2 meals per day feeding schedule with the afternoon meal at 2:30 pm. Complete daily urine samples were collected throughout the study period.

Processing of plasma samples from metabolic studies

Plasma was isolated by low speed centrifugation of the timed blood samples. An aliquot of plasma was subjected to radiolabel quantification of ^{125}I using a gamma counter. Another aliquot of plasma was run on 4–30% non-denaturing gradient gels, as described above, and the regions corresponding to large (10.4–12.2 nm), medium (8.2–10.4 nm), and small (7.2–8.2 nm) and pre-beta (<7.2 nm) particles were sliced and quantified for ^{125}I radioactivity in the gamma counter. The gel slices were taken according to a template that was calibrated using the migration of

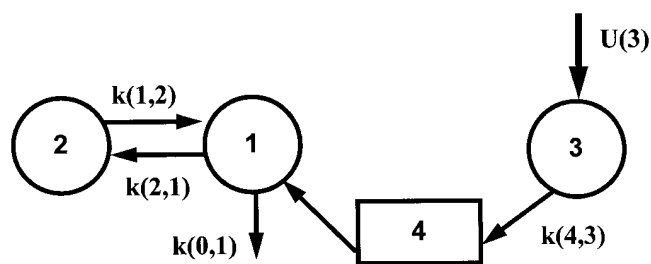


Fig. 2. Model used for analysis of large HDL apoA-I kinetic data. This model is characterized by a single plasma compartment of large HDL, C(1), that exchanges with an extravascular compartment, C(2). The model includes a noncirculating compartment of large HDL, C(3). ApoA-I in this compartment, C(3), passes through a delay compartment, C(4), before entering the plasma compartment. All injected radiolabeled large LpAI is distributed between the plasma compartment, C(1), and the noncirculating compartment, C(3). In this model the input or production, U(3), of apoA-I is into the noncirculating compartment, C(3), and assumes that all large HDL is derived from C(3).

Pharmacia high molecular weight protein standards and a prestained (Sudan Black) control plasma. The inter-assay coefficient of variation for radiolabel in large, medium, and small LpAI for the same plasma sample run multiple times was <5%.

A duplicate non-denaturing gradient gel of plasma samples from each recipient animal was run to determine the relative distribution of apoA-I among the large, medium, and small particles. Electrophoretic transfer and blotting with anti-apoA-I was performed as described above. The stained blot was scanned with a laser densitometer and the regions corresponding to large, medium, small, and pre-beta particles (described above) were cut and weighed to calculate a fractional apoA-I distribution among the HDL particles. The fractional distribution was multiplied times the apoA-I concentration in the plasma sample, determined by ELISA. The specific radioactivity of each size range of HDL was then calculated as cpm/ μ g from the cpm and μ g value for apoA-I in each size fraction. The gradient gel of plasma includes apoA-II-containing particles and therefore the fractional distribution of apoA-I mass in large HDL by this method does not include LpAI alone. Further, some tracer LpAI was converted to LpAI:AII particles after injection during the turnover

studies. Therefore, the kinetic studies trace apoA-I in large HDL, both large LpAI and large LpAI:AII.

Kinetic analysis

Analysis of the apoA-I specific activity was completed using the SAAM II program (SAAM Institute, Seattle, WA). A previously published model of plasma HDL kinetics (37) did not provide a good fit of the apoA-I specific activity in large HDL and was not consistent with the kinetic data of this study. Therefore, a model was developed to describe the large HDL specific activity data and is shown in **Fig. 2**. This model is characterized by a single plasma compartment of large HDL, C(1), that exchanges with an extravascular compartment, C(2). The model includes a noncirculating compartment of large HDL, C(3). ApoA-I in this compartment, C(3), passes through a delay compartment, C(4), before entering the plasma compartment. All injected radiolabeled large LpAI is distributed between the plasma compartment, C(1) and the noncirculating compartment, C(3). In this model the input or production, U(3), of apoA-I is into the noncirculating compartment, C(3), and assumes that all large HDL is derived from C(3).

Data analysis and statistics

Data are reported for individual monkeys and as mean \pm standard deviation for each group. A Student's *t*-test was used to determine whether significant differences in the data existed between the low and high HDL animals.

RESULTS

Plasma concentrations of lipids, lipoproteins, and apolipoproteins are given in **Table 1**. The low HDL group had HDL cholesterol concentrations that were one-third that of the high HDL group, and total plasma cholesterol concentrations that were twice that of the high HDL group. Triglyceride concentrations were similar between both groups of animals. ApoA-I and apoA-II concentrations were twice as high in the high HDL group compared to the low group, whereas the opposite trend was observed for plasma apoE concentrations.

The distribution of apoA-I among LpAI particles of different size is shown in **Table 2**. In the high HDL group the

TABLE 1. Plasma concentration of lipids, lipoproteins and apolipoproteins

| Group, Animal # | TPC | TG | HDL-C | ApoA-I | ApoA-II | ApoE |
|-----------------|--------------|------------|--------------|--------------|----------------|----------------|
| | <i>mg/dl</i> | | | | | |
| Low HDL | | | | | | |
| 765 | 563 | 26 | 42 | 277 | 8.0 | 17.0 |
| 768 | 542 | 13 | 27 | 124 | 3.5 | 12.2 |
| 771 | 432 | 19 | 52 | 255 | 11.6 | 9.6 |
| Mean \pm SD | 512 \pm 70 | 19 \pm 7 | 40 \pm 13 | 219 \pm 83 | 7.7 \pm 4.1 | 12.9 \pm 3.6 |
| High HDL | | | | | | |
| 738 | 220 | 24 | 100 | 382 | 21.2 | 4.5 |
| 752 | 204 | 21 | 98 | 492 | 19.5 | 5.1 |
| 777 | 319 | 18 | 161 | 413 | 11.9 | 4.9 |
| Mean \pm SD | 248 \pm 62 | 21 \pm 3 | 120 \pm 35 | 429 \pm 58 | 17.5 \pm 5.0 | 4.8 \pm 0.3 |
| <i>P</i> value | 0.001 | NS | 0.02 | 0.02 | 0.06 | 0.02 |

Total plasma cholesterol (TPC), HDL cholesterol (HDL-C), and triglyceride (TG) concentrations are the mean values ($n = 27$) for each animal from months 3–68 on the experimental diet. Apolipoprotein values, determined by ELISA, were measured after 45 months of the experimental diet. NS indicates not significant.

TABLE 2. Distribution of apoA-I in large, medium, and small LpAI particles

| Group, Animal # | Plasma ApoA-I | | |
|-----------------|------------------|-------------------|-------------------|
| | Large LpAI | Medium LpAI | Small LpAI |
| | <i>mg/dl</i> | | |
| Low HDL | | | |
| 765 | 6.8 | 15.3 | 15.2 |
| 768 | 2.3 | 1.8 | 2.7 |
| 771 | 9.5 | 27.0 | 23.0 |
| Mean ± SD | 6.2 ± 3.6 (18%) | 14.7 ± 12.6 (43%) | 13.6 ± 10.2 (39%) |
| High HDL | | | |
| 738 | 41.5 | 30.8 | 16.4 |
| 752 | 43.4 | 49.3 | 44.1 |
| 777 | 58.9 | 62.2 | 46.6 |
| Mean ± SD | 47.9 ± 9.5 (37%) | 47.4 ± 15.8 (36%) | 35.7 ± 16.8 (27%) |
| P value | 0.002 | 0.05 | NS |

Values were determined by apoA-I ELISA on LpAI fractions isolated by size-exclusion and immunoaffinity chromatography. Values in parentheses are the mean percentage apoA-I distribution among LpAI of different size; NS, not significant.

distribution of apoA-I was skewed towards large particles (37% of total apoA-I in large LpAI), whereas for the low HDL group, only 18% of apoA-I in LpAI was associated with the large particles. Total apoA-I concentration in large LpAI particles was 8 times greater in the high HDL group compared with the low HDL group and apoA-I concentration in medium LpAI particles was 3 times greater in the high HDL group. Although a similar trend was observed in small LpAI, the difference in apoA-I concentration in this fraction between the two groups of animals did not reach statistical significance.

The distribution of apoA-I in LpAI:AII particles as a function of size is shown in **Table 3**. The concentration of apoA-I in the LpAI:AII particles in the high HDL group was approximately twice that of the low HDL group for all

TABLE 3. Distribution of apoA-I in large, medium, and small LpAI:AII particles

| Group, Animal # | ApoA-I | | |
|-----------------|-------------------|-------------------|--------------------|
| | Large LpAI:AII | Medium LpAI:AII | Small LpAI:AII |
| | <i>mg/dl</i> | | |
| Low HDL | | | |
| 765 | 30.5 | 56.9 | 57.8 |
| 768 | 11.9 | 30.0 | 58.5 |
| 771 | 20.7 | 41.7 | 85.4 |
| Mean ± SD | 21.0 ± 9.3 (16%) | 42.9 ± 13.5 (33%) | 67.2 ± 15.7 (51%) |
| High HDL | | | |
| 738 | 49.9 | 96.6 | 116.1 |
| 752 | 37.4 | 88.2 | 90.6 |
| 777 | 58.4 | 89.3 | 145.7 |
| Mean ± SD | 48.6 ± 10.6 (19%) | 91.4 ± 4.6 (35%) | 117.5 ± 27.6 (46%) |
| P value | 0.03 | 0.004 | 0.05 |

Values were determined by apoA-I ELISA on LpAI:AII fractions isolated by size-exclusion and immunoaffinity chromatography. Values in parentheses are the mean percentage apoA-I distribution among LpAI:AII of different size.

TABLE 4. Chemical composition of the apoA-I-containing particles as percent of total mass

| HDL Fraction | Protein | Phospholipid | Free Cholesterol | Cholesteryl Ester | Triglyceride |
|--------------|---------|--------------|------------------|-------------------|--------------|
| Lg LpAI | 41.7 | 33.9 | 4.2 | 18.7 | 1.4 |
| Lg LpAI:AII | 42.0 | 33.4 | 3.9 | 17.6 | 3.1 |
| Md LpAI | 56.9 | 22.6 | 1.8 | 16.8 | 1.9 |
| Md LpAI:AII | 55.0 | 24.4 | 1.8 | 17.7 | 1.1 |
| Sm LpAI | 71.3 | 11.6 | 1.4 | 14.2 | 1.5 |
| Sm LpAI:AII | 62.9 | 20.1 | 1.4 | 14.8 | 0.7 |

Values represent a single determination of large (Lg) LpAI and LpAI:AII from an animal with high HDL concentrations and a single determination medium (Md) and small (Sm) LpAI and LpAI:AII from an animal with low HDL concentrations.

three particle sizes. For both groups of animals, the distribution of apoA-I among large, medium, and small LpAI:AII was similar. It is notable that more apoA-I is distributed in LpAI:AII particles (**Table 3**) than in LpAI particles (**Table 2**). In the high HDL group, 24.9% of total apoA-I was associated with large HDL, both LpAI and LpAI:AII, compared with 16.1% in the low group.

The chemical composition of LpAI and LpAI:AII is given in **Table 4**. The compositions of LpAI were similar to those of LpAI:AII in the large and medium particles. The small LpAI particles were slightly more enriched in protein and contained less phospholipid compared to the small LpAI:AII particles. As particle size increased the phospholipid, free cholesterol and cholesteryl ester as a percentage of the total mass increased, whereas protein decreased.

Kinetic studies of large HDL

The radiolabeled tracer for the kinetic studies was LpAI. The injected dose contained 87% large LpAI particles, 10% medium LpAI particles, and 3% small LpAI particles as analyzed on gradient gels at the time of injection. Analysis of the tracer LpAI before re-injection indicated that only apoA-I was present in the tracer. No apoA-II or apoE was detected in the LpAI tracer. After the injection of the tracer LpAI, 30–40% of the injected radiolabeled large LpAI tracer was converted to large LpAI:AII during the turnover study. **Figure 3** shows the plasma die-away of large, medium and small HDL specific activity after the injection of radiolabeled large LpAI in a monkey with high HDL concentration. As determined by non-denatured gradient gel electrophoresis of the first plasma sample collected during the kinetic studies, the distribution of injected tracer radioactivity in large, medium, and small HDL was unchanged with no significant transfer of tracer apoA-I radioactivity between HDL particles of differing size before the first plasma sample was collected. During the turnover study there was no evidence of significant transfer of radioactivity from large HDL to medium or small HDL suggesting that there is no conversion of large HDL to medium or small HDL. Furthermore, there was no evidence of transfer of radiolabeled apoA-I to apoB-containing lipoproteins and no significant free apoA-I in plasma. Because the specific activity of the medium and small HDL was low throughout the turnover study and be-

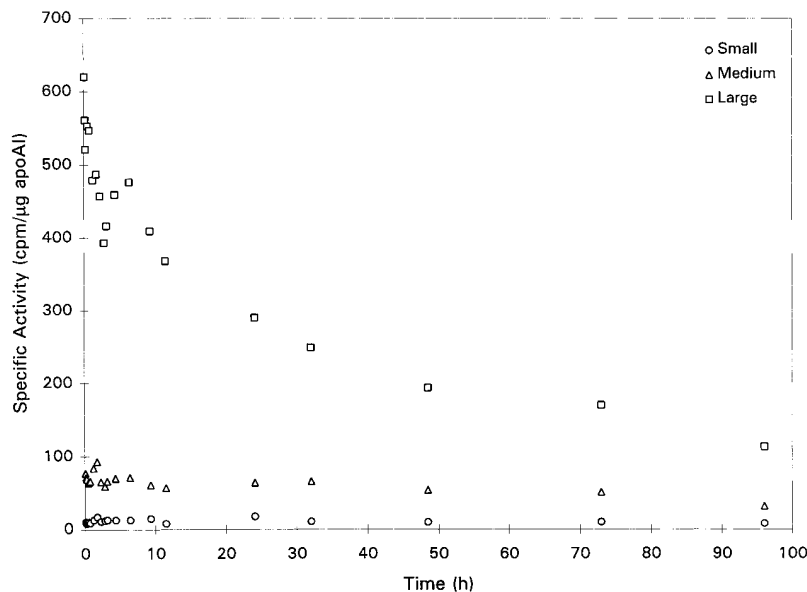


Fig. 3. Specific activity for apoA-I in large (squares), medium (triangles), and small HDL (circles) after the injection of large LpAI in a representative African green monkey consuming an atherogenic diet. Experimental data represent specific activity expressed as CPM/microgram apoA-I.

cause there was no evidence of transfer of radiolabeled apoA-I among HDL particles of differing sizes or to apoB-containing particles after the injection of radiolabeled large LpAI, we directed our modelling efforts to the kinetics of large HDL only. Thus, in this report, the turnover of apoA-I in only large HDL, consisting of both large LpAI and large LpAI:AII particles, will be examined.

The plasma specific activity of apoA-I in large HDL after the injection of radiolabeled large LpAI in a representative monkey from the high HDL group is shown in **Fig. 4** and in a representative monkey from the low HDL group in **Fig. 5**. Only 60% of the injected tracer dose could be accounted for in the plasma volume. However, in both the high and low HDL groups, an increase in specific activity in large HDL was observed after the start of the initial component of the die-away curve, but before the start of the slow component of the die-away curve, resulting in a delayed peak in

specific activity 2.99 ± 1.15 h after injection of tracer. The delay peak occurred 3.34 ± 0.43 h after injection of tracer in the high HDL group and 2.09 ± 0.51 h after injection in the low HDL group. The delayed peak was not an artifact of the turnover method itself and occurred in each animal studied. There was no evidence that the delayed peak was due to a change in apoA-I concentration in large HDL. The coefficient of variation of whole plasma apoA-I concentration during the kinetic studies was no more than 18% and the variation in measured plasma apoA-I concentration during the kinetic studies was random and did not account for the delayed peak. The change in total radioactivity per milliliter of plasma, as a measure independent of the apoA-I concentration, paralleled the change in specific activity. There was no evidence that the delayed peak was the result of partial extravasation of tracer into subcutaneous or extravascular tissue during the injection of the tracer dose

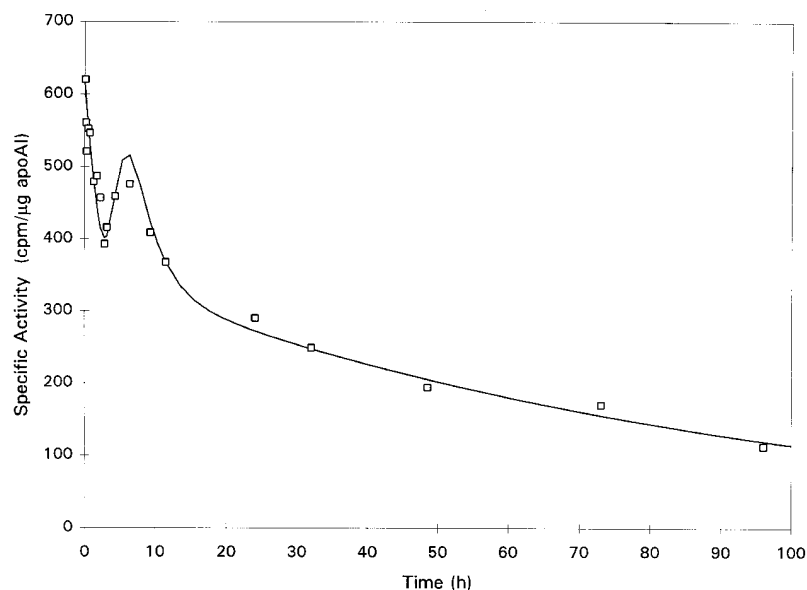


Fig. 4. Specific activity for apoA-I in large HDL (squares) after the injection of large LpAI in a representative African green monkey from the high HDL group. Solid lines are the computer-predicted values. Experimental data represent specific activity expressed in CPM/microgram apoA-I.

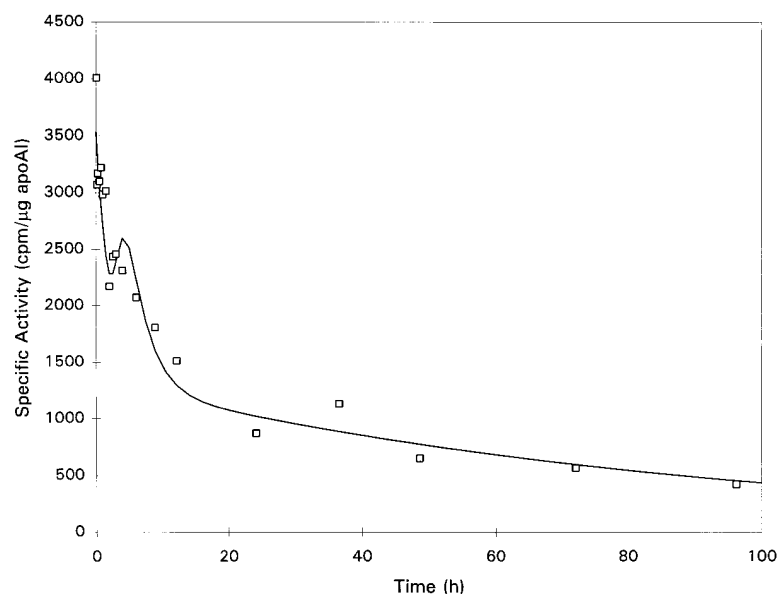


Fig. 5. Specific activity for apoA-I in large HDL (squares) after the injection of large LpAI in a representative African green monkey from the low HDL group. Solid lines are the computer-predicted values. Experimental data represent specific activity expressed as CPM/microgram apoA-I.

which might produce a delayed leakage of tracer material into plasma after the start of the turnover study. In addition, there was no evidence that the delayed rise in specific activity was an artifact of the re-isolation of large, medium, and small HDL from plasma samples collected during the turnover study.

A previously published model of plasma HDL kinetics (37) did not provide a good fit when applied to the apoA-I specific activity in large HDL alone and was not consistent with the delayed peak in specific activity. We hypothesized that the delayed peak in specific activity may be produced by the return to circulating plasma of large HDL particles that were temporarily sequestered outside the circulating plasma after the injection of the tracer. The computer-predicted values generated by the kinetic model that incorporates this hypothesized mechanism (represented by the lines) are consistent with the experimental turnover data (represented by the data points) as seen in Figs. 4 and 5. The rate constants of the large HDL apoA-I kinetic model for the high and low HDL groups are shown in **Table 5**. This model accounts for all radioactivity injected during the kinetic studies with 60% distributed to the circulating pool, C(1), and 40% distributed to the non-circulating pool,

TABLE 5. Rate constants for large HDL apoA-I model

| Group, Animal # | k(0, 1) | k(1, 2) | k(2, 1) | k(4, 3) |
|-----------------|-----------|----------|-----------|------------|
| Low HDL | | | | |
| 765 | 1.04 (5) | 2.14 (7) | 5.30 (13) | 42.84 (12) |
| 768 | 1.02 (5) | 2.08 (6) | 7.43 (8) | 41.61 (13) |
| 771 | 1.04 (5) | 2.12 (7) | 3.14 (34) | 42.33 (12) |
| High HDL | | | | |
| 738 | 0.96 (11) | 1.88 (6) | 4.98 (7) | 6.77 (14) |
| 752 | 1.69 (6) | 1.99 (5) | 4.16 (9) | 4.89 (21) |
| 777 | 0.79 (8) | 1.93 (6) | 3.35 (10) | 4.63 (11) |

Units are pools per day. Numbers in parentheses are coefficient of variation or percent standard deviation, expressed as a percentage, for each rate constant.

C(3), and accounts for all radioactivity excreted in the urine (97% of the injected tracer dose).

Although the high HDL group had significantly higher concentrations of large HDL and apoA-I in the large HDL fraction, the model-predicted fractional catabolic rate of apoA-I in large HDL was not significantly different in the low and high HDL groups (**Table 6**). In contrast, the mean production rate of apoA-I in large HDL was a 4-fold greater ($P < 0.009$) in the high HDL group.

DISCUSSION

The major anti-atherogenic portion of HDL is hypothesized to be LpAI which is increased in individuals with elevated HDL and low risk for CAD. For example, there is a clear sex difference in the incidence of CAD across age in

TABLE 6. Model-predicted metabolic parameters of large HDL apoA-I after injection of radiolabeled large LpAI

| Group, Animal # | ApoA-I in Large HDL | FCR | Production Rate of ApoA-I in Large HDL |
|-----------------|---------------------|----------------|--|
| | mg/dl | pools/day | mg/day |
| Low HDL | | | |
| 765 | 37.30 | 1.04 | 38.79 |
| 768 | 14.17 | 1.02 | 14.45 |
| 771 | 30.19 | 1.04 | 31.39 |
| Mean \pm SD | 27.2 \pm 11.8 | 1.03 \pm .01 | 28.21 \pm 12.5 |
| High HDL | | | |
| 738 | 91.42 | 0.96 | 87.76 |
| 752 | 80.81 | 1.69 | 136.57 |
| 777 | 119.50 | 0.79 | 94.41 |
| Mean \pm SD | 97.2 \pm 19.9 | 1.15 \pm .48 | 106.25 \pm 26.5 |
| P value | 0.006 | NS | 0.009 |

Plasma apoA-I concentration in large HDL and production rate of apoA-I in large HDL are significantly greater in the High group. No difference was found comparing the fractional catabolic rate between the Low and High groups.

Western societies. Women, who have on average a 10 year delay in onset of CAD compared with men, have higher LpAI concentrations than men attributable, in part, to higher concentrations of large LpAI. In cholesterol-fed African green monkeys, higher HDL concentration has been shown to be inversely correlated to coronary artery atherosclerosis extent (10, 11). In this group of cholesterol-fed African green monkeys, higher HDL concentration was associated with higher concentrations of apoA-I in large HDL particles as a fraction of total apoA-I. This increase in apoA-I in large HDL was attributable to a significant increase in the production rate of apoA-I in large HDL, but not to a decrease in the fractional catabolic rate. Increased production of large HDL accounted for the increased large HDL concentration in monkeys with low risk of CAD.

Much of our understanding of the catabolism of HDL is derived from turnover studies in which the HDL tracer was isolated by ultracentrifugation. However, ultracentrifugation causes structural changes in HDL particles resulting from the shedding of apoA-I from the particles. After ultracentrifugation, the apoA-I content of HDL may be as little as 65% of the pre-ultracentrifugation content (13). Thus, HDL tracers isolated by ultracentrifugation may no longer accurately represent HDL in circulation *in vivo* which confounds the interpretation of the kinetics of such tracers. The method used to overcome this methodological limitation in the present study was to avoid the use of ultracentrifugation during the isolation of HDL tracers and during the processing of plasma samples collected in the course of the turnover study. This study is believed to be the first in monkeys to use such methods and demonstrates that large LpAI can be isolated and radiolabeled for reinjection studies without exposing the tracer to ultracentrifugation. The integrity of the large LpAI tracer, as analyzed on nondenaturing gradient gels, was well maintained.

Some previous kinetic studies have described a subpopulation of apoA-I which is not tightly associated with HDL tracers that have been subjected to ultracentrifugation (13). This subpopulation of apoA-I has been described to transfer rapidly from the HDL tracer to other lipoproteins in plasma after reinjection. There was no evidence in the present study of rapid transfer of radioactivity from the large LpAI tracer to smaller HDL in a fashion analogous to the rapid transfer of radiolabeled apoA-I to other particles described in studies using HDL tracers isolated by ultracentrifugation. Although an explanation for the discordance of the current study on this point cannot be fully determined from the present observations, ultracentrifugation is known to cause structural changes and dissociation of apoA-I from HDL particles that may alter metabolic pathways or the metabolic behavior of HDL tracers isolated by ultracentrifugation. During the course of these studies, for example, we found that the large LpAI fraction was particularly susceptible to disruption by ultracentrifugation, but remained fully intact during the immunoaffinity isolation procedure used here. The data of this study demonstrate that after reinjection, the radioactive

apoA-I of the tracer remained associated with large HDL throughout the turnover study, clearly indicating that no significant transfer of the radiolabeled apoA-I from the large LpAI tracer to intermediate and smaller HDL fractions occurred. Further, no significant metabolic conversion of large HDL to medium or small HDL (including pre- β HDL) occurred. This is a new observation that is unique among HDL turnover studies of which we are aware, and suggests that the mode of isolation of the HDL tracer particles is important in determining the outcome of the study. Our observation supports the hypothesis that large HDL particles are mature, metabolically stable particles. Our analysis assumes that large HDL particles are cleared from plasma as a whole entity. This assumption is supported by the lack of evidence that large HDL was converted to smaller HDL particles during the turnover studies. We hypothesize that if large HDL particles are metabolized within the plasma by the removal of constituents of the large HDL, including apoproteins, then smaller HDL particles should be produced in plasma as a result of this process and some of the smaller HDL particles produced during this hypothetical process should be radiolabeled. Large HDL particles are mature, metabolically stable in that they are removed directly from plasma without conversion to intermediate particles and thus, large HDL may be the final product of the HDL metabolic pathway. Because high concentrations of large HDL are associated with low risk for CAD and because the catabolic rate of large HDL does not account for differences in concentration of HDL and subsequent CAD risk, the rate of production of large HDL is possibly a measure of the rate of reverse cholesterol transport. Thus, increased plasma concentration of large HDL that confers decreased risk for CAD may be the legacy of accelerated reverse cholesterol transport.

Although great care was taken to isolate a homogeneous tracer, large LpAI, for the kinetic studies, heterogeneity was observed. First, 30–40% of the injected large LpAI tracer was converted to large LpAI:AI particles early during the turnover study. Because there was no evidence that radiolabeled apoA-I is transferred from large HDL tracers to other smaller HDL particles during these kinetic studies, as discussed above, the conversion of radiolabeled large LpAI tracer to large LpAI:AI particles during the turnover study may be the result of the gain of an apoA-II molecule(s) by the tracer large LpAI rather than the transfer of a radiolabeled apoA-I molecule from large LpAI tracer to an unlabeled large LpAI:AI particle. Only radiolabeled apoA-I in large HDL was traced in these turnover studies and the turnover of other constituents of HDL, such as apoA-II and cholesteryl ester, was not evaluated.

Second, in the present study only 60% of the injected large LpAI tracer could be accounted for in the plasma 5 min after the start of the turnover study. The remaining 40% of the injected large LpAI tracer was distributed to a noncirculating compartment. Several hours after the injection of the tracer, an increase in the plasma specific activity of apoA-I in large HDL was observed which we hypothesize is due to the re-entry of large LpAI tracer from

the noncirculating pool into the circulating plasma pool. This reproducible observation was not apparently an artifact of the injection process or sampling process after reinjection in this study nor due to a change in concentration of apoA-I in large HDL during this period of the turnover studies. In the kinetic model, all injected tracer material was distributed to the plasma compartment and the noncirculating compartment at the start of the turnover study. The delay time is a measure of the average time a particle will spend in the delay compartment before appearing in the plasma compartment. The fraction of the injected dose that was distributed to the noncirculating pool spends on average 2.99 h before appearing in the plasma.

Because the delayed peak was observed in both the low and high group, we hypothesized that this kinetic evidence of a noncirculating pool must have a biologically plausible explanation. The anatomical location of the hypothesized noncirculating compartment of large HDL apoA-I cannot be determined from the present observations but may be surmised on the basis of previously published observations regarding the distribution of HDL. That is, the laminar blood flow through minute peripheral vessels is known to cause red blood cells to segregate in the more rapidly moving central stream whereas plasma tends to move more sluggishly near the vessel wall, a process known as margination. HDL is not confined to the vascular space because the permeability characteristics of the vascular endothelium discriminate against larger in favor of smaller particles. Whole HDL particles can cross the vascular endothelium and are found in lymph and in the subendothelial spaces of arteries. The plasma decay curves from reinjected radiolabeled lipoproteins are known to underestimate the transport of lipoproteins from plasma into lymph. Thus, we hypothesize that the noncirculating compartment represents HDL particles sequestered from the circulating plasma compartment in the margins of peripheral vessels, within the porous pathways of the vascular endothelium and in the subendothelial spaces of arteries. The HDL particles sequestered in the noncirculating pool return to the circulating plasma before they are catabolized.

Both the noncirculating compartment, C(3), and the extravascular compartment, C(2), are necessary to model the specific activity of apoA-I in large HDL in plasma. At present the existence of C(3) and C(2) as separate compartments is based solely on the kinetic behavior of tracer large LpAI distributed to these compartments. The kinetics of C(3) and C(2) are quite distinct. The average residence time of particles in C(3) is less than 1 h while that in C(2) is more than 100 h. The noncirculating compartment, in theory, may be conceptualized as HDL particles that are in close proximity with cells, a needed occurrence during reverse cholesterol transport of excess cellular cholesterol to HDL, which then return to the circulating compartment. Although the kinetic data in this study are limited to the turnover of radiolabeled apoA-I in large HDL and we are unable to directly demonstrate that the tracer HDL particles acquired additional cholesterol while distributed to the noncirculating pool, the

observations made during these studies are consistent with the hypothesis that large HDL may move between the circulating and non-circulating pools.

In this group of cholesterol-fed African green monkeys, higher HDL concentration was associated with higher concentrations of apoA-I in large HDL particles as a fraction of total apoA-I. This increase in apoA-I in large HDL was attributable to a significant increase in the production rate of apoA-I in large HDL, but not to a decrease in the fractional catabolic rate. Increased production of large HDL accounted for the increased large HDL concentration in monkeys with low risk of CAD. The animals with higher production rates of apoA-I in large HDL also had higher plasma concentrations of apoA-I in small and medium HDL, suggesting the possibility that apoA-I in smaller HDL may be, in part, the substrate for apoA-I in large HDL. Large HDL particles are distributed to the circulating plasma and to a noncirculating pool that we hypothesize to be in close physical proximity with cells that would allow the transfer of excess cellular cholesterol to HDL particles during reverse cholesterol transport. ■■

Supported in part by National Institutes of Health grants HL-49373, HL-24736, RR-02176, and HL-49110.

Manuscript received 8 December 1997, in revised form 1 May 1998, and in revised form 25 June 1998.

REFERENCES

1. Eisenberg, S. 1984. High density lipoprotein metabolism. *J. Lipid Res.* **25**: 1017-1058.
2. Blanche, P. J., E. L. Gong, T. M. Forte, and A. V. Nichols. 1981. Characterization of human high-density lipoproteins by gradient gel electrophoresis. *Biochim. Biophys. Acta.* **665**: 408-419.
3. Anderson, D. W., A. V. Nichols, S. S. Pan, and F. T. Lindgren. 1978. High density lipoprotein distribution. Resolution and determination of three major components in a normal population sample. *Atherosclerosis.* **29**: 161-179.
4. Anderson, D. W., A. V. Nichols, T. M. Forte, and F. T. Lindgren. 1977. Particle distribution of human serum high density lipoproteins. *Biochim. Biophys. Acta.* **493**: 55-68.
5. Noble, R. P., F. T. Hatch, J. A. Mazrimas, F. T. Lindgren, L. C. Jensen, and G. L. Adamson. 1969. Comparison of lipoprotein analysis by agarose gel and paper electrophoresis with analytical ultracentrifugation. *Lipids.* **4**: 55-59.
6. Cheung, M. C., and J. J. Albers. 1982. Distribution of high density lipoprotein particles with different apoprotein composition: particles with A-I and A-II and particles with A-I but no A-II. *J. Lipid Res.* **23**: 747-753.
7. Pieters, M. N., D. Schouten, and T. J. C. Van Berkel. 1994. In vitro and in vivo evidence for the role of HDL in reverse cholesterol transport. *Biochim. Biophys. Acta.* **1225**: 125-134.
8. Gordon, D. J., and B. M. Rifkind. 1989. High-density lipoprotein: the clinical implications of recent studies. *N. Engl. J. Med.* **321**: 1311-1316.
9. Fielding, C. J., and P. E. Fielding. 1995. Molecular physiology of reverse cholesterol transport. *J. Lipid Res.* **36**: 211-228.
10. Quinet, E., A. Tall, R. Ramakrishnan, and L. Rudel. 1991. Plasma lipid transfer protein as a determinant of the atherogenicity of monkey plasma lipoproteins. *J. Clin. Invest.* **87**: 1559-1566.
11. Rudel, L. L., M. G. Bond, and B. C. Bullock. 1985. LDL heterogeneity and atherosclerosis in nonhuman primates. *Ann. NY Acad. Sci.* **454**: 248-253.
12. Rubin, E. M., R. M. Krauss, E. A. Spangler, J. G. Verstuyft, and S. M. Clift. 1991. Inhibition of early atherogenesis in transgenic mice by human apolipoprotein A-I. *Nature.* **353**: 265-267.

13. Kunitake, S. T., and J. P. Kane. 1982. Factors affecting the integrity of high density lipoproteins in the ultracentrifuge. *J. Lipid Res.* **23**: 936–940.
14. Cheung, M. C., and J. J. Albers. 1984. Characterization of lipoprotein particles isolated by immunoaffinity chromatography. Particles containing A-I and A-II and particles containing A-I but no A-II. *J. Biol. Chem.* **259**: 12201–12209.
15. Puchois, P., A. Kandoussi, P. Fievet, J. L. Fourrier, M. Bertrand, and E. Koren. 1987. Apolipoprotein A-I-containing lipoproteins in coronary artery disease. *Atherosclerosis.* **68**: 35–40.
16. Schultz, J. R., J. G. Verstuyft, E. L. Gong, A. V. Nichols, and E. M. Rubin. 1993. Protein composition determines the anti-atherogenic properties of HDL in transgenic mice. *Nature.* **365**: 762–764.
17. Fruchart, J. C., G. Ailhaud, and J. M. Bard. 1993. Heterogeneity of high density lipoprotein particles. *Circulation.* **87** (Suppl.): III22–III27.
18. Castro, G., L. P. Nihoul, C. Dengremont, C. De Geitère, B. Delfly, A. Tailleux, C. Fievet, N. Duverger, P. Denèfle, J. C. Fruchart, and E. M. Rubin. 1997. Cholesterol efflux, lecithin:cholesterol acyltransferase activity, and pre- β particle formation by serum from human apolipoprotein A-I and apolipoprotein A-II apolipoprotein A-II transgenic mice consistent with the latter being less effective for reverse cholesterol transport. *Biochemistry.* **36**: 2243–2249.
19. Rader, D. J., G. Castro, L. A. Zech, J. C. Fruchart, and H. B. Brewer, Jr. 1991. In vivo metabolism of apolipoprotein A-I on high density lipoprotein particles LpA-I and LpA-I, A-II. *J. Lipid Res.* **32**: 1849–1859.
20. Duverger, N., D. Rader, and H. B. Brewer, Jr. 1994. Distribution of subclasses of HDL containing apoA-I without apoA-II (LpA-I) in normolipidemic men and women. *Arterioscler. Thromb.* **14**: 1594–1599.
21. Horowitz, B. S., I. J. Goldberg, J. Merab, T. M. Vanni, R. Ramakrishnan, and H. N. Ginsberg. 1993. Increased plasma and renal clearance of an exchangeable pool of apolipoprotein A-I in subjects with low levels of high density lipoprotein cholesterol. *J. Clin. Invest.* **91**: 1743–1752.
22. Brinton, E. A., S. Eisenberg, and J. L. Breslow. 1994. Human HDL cholesterol levels are determined by apoA-I fractional catabolic rate, which correlates inversely with estimates of HDL particle size: effects of gender, hepatic and lipoprotein lipases, triglyceride and insulin levels, and body fat distribution. *Arterioscler. Thromb.* **14**: 707–720.
23. Rudel, L. L., C. Deckelman, M. Wilson, M. Scobey, and R. Anderson. 1994. Dietary cholesterol and down-regulation of cholesterol 7 α -hydroxylase and cholesterol absorption in African green monkeys. *J. Clin. Invest.* **93**: 2463–2472.
24. Parks, J. S., and L. L. Rudel. 1979. Isolation and characterization of high density lipoprotein apoproteins in the non-human primate (vervet). *J. Biol. Chem.* **254**: 6716–6723.
25. Parks, J. S. and L. L. Rudel. 1980. Detection of immunological heterogeneity of an isolated, purified protein (vervet apolipoprotein A-I). *Biochim. Biophys. Acta.* **618**: 327–336.
26. Koritnik, D. L., and L. L. Rudel. 1983. Measurement of apolipoprotein A-I concentration in nonhuman primate serum by enzyme-linked immunosorbent assay (ELISA). *J. Lipid Res.* **24**: 1639–1645.
27. Lowry, O. H., N. J. Rosebrough, A. L. Farr, and R. J. Randall. 1951. Protein measurement with the Folin phenol reagent. *J. Biol. Chem.* **193**: 265–275.
28. Rouser, G., S. Fleischer, and A. Yamamoto. 1970. Two-dimensional thin-layer chromatographic separation of polar lipids and determination of phospholipids by phosphorus analysis of spots. *Lipids.* **5**: 494–496.
29. Carr, T. P., C. J. Andresen, and L. L. Rudel. 1993. Enzymatic determination of triglyceride, free cholesterol, and total cholesterol in tissue lipid extracts. *Clin. Biochem.* **26**: 39–42.
30. Bligh, E. G., and W. J. Dyer. 1959. A rapid method of total lipid extraction and purification. *Can. J. Biochem. Physiol.* **37**: 911–917.
31. Auerbach, B. J., and J. S. Parks. 1989. Lipoprotein abnormalities associated with lipopolysaccharide-induced lecithin:cholesterol acyltransferase and lipase deficiency. *J. Biol. Chem.* **264**: 10264–10270.
32. Rainwater, D. L., P. H. Moore, Jr., W. R. Shelledy, T. D. Dyer, and S. H. Slifer. 1997. Characterization of a composite gradient gel for the electrophoretic separation of lipoproteins. *J. Lipid Res.* **38**: 1261–1266.
33. McFarlane, A. A. 1958. Efficient trace labelling of proteins with iodine. *Nature.* **182**: 53–57.
34. Bilheimer, D. W., S. Eisenberg, and R. I. Levy. 1972. The metabolism of very low density lipoprotein proteins. I. Preliminary in vitro and in vivo observations. *Biochim. Biophys. Acta.* **260**: 212–221.
35. Swaney, J. B. 1986. Use of cross-linking reagents to study lipoprotein structure. *Methods Enzymol.* **128**: 613–626.
36. Marzetta, C. A., F. L. Johnson, L. A. Zech, D. M. Foster, and L. L. Rudel. 1989. Metabolic behavior of hepatic VLDL and plasma LDL apoB-100 in African green monkeys. *J. Lipid Res.* **30**: 357–370.
37. Blum, C. B., R. I. Levy, S. Eisenberg, M. Hall, R. H. Goebel, and M. Berman. 1977. High density lipoprotein metabolism in man. *J. Clin. Invest.* **60**: 795–807.